

Lawrence Berkeley National Laboratory

Recent Work

Title

STUDY OF THE CHARGE-EXCHANGE REACTION (d,2He)

Permalink

<https://escholarship.org/uc/item/8v3795np>

Author

Jahn, R.

Publication Date

1977-10-01

Submitted to Physical Review C

uc-34c
LBL-6589
Preprint 91

STUDY OF THE CHARGE-EXCHANGE REACTION ($d, {}^2\text{He}$)

R. Jahn, D. P. Stahel, G. J. Wozniak, and
Joseph Cerny

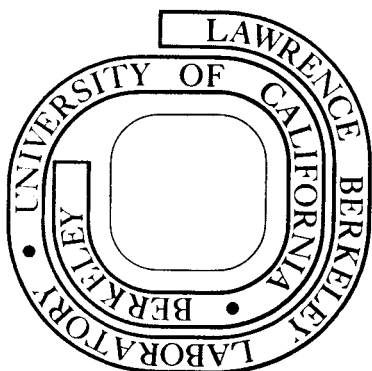
October 1977

RECEIVED
LAWRENCE
BERKELEY LABORATORY
DEC 15 1977
LIBRARY AND
DOCUMENTS SECTION

Prepared for the U. S. Department of Energy
under Contract W-7405-ENG-48

For Reference

Not to be taken from this room



LBL-6589
91

DISCLAIMER

This document was prepared as an account of work sponsored by the United States Government. While this document is believed to contain correct information, neither the United States Government nor any agency thereof, nor the Regents of the University of California, nor any of their employees, makes any warranty, express or implied, or assumes any legal responsibility for the accuracy, completeness, or usefulness of any information, apparatus, product, or process disclosed, or represents that its use would not infringe privately owned rights. Reference herein to any specific commercial product, process, or service by its trade name, trademark, manufacturer, or otherwise, does not necessarily constitute or imply its endorsement, recommendation, or favoring by the United States Government or any agency thereof, or the Regents of the University of California. The views and opinions of authors expressed herein do not necessarily state or reflect those of the United States Government or any agency thereof or the Regents of the University of California.

STUDY OF THE CHARGE-EXCHANGE REACTION $(d, {}^2\text{He})^\dagger$

R. Jahn*, D. P. Stahel, G. J. Wozniak and Joseph Cerny

Lawrence Berkeley Laboratory
 and Department of Chemistry
 University of California
 Berkeley, California 94720

October 1977

ABSTRACT

A ${}^2\text{He}$ detection system has been used to investigate the charge-exchange reaction $(d, {}^2\text{He})$ at 55 MeV on ${}^6\text{Li}$, ${}^{10}\text{B}$, and ${}^{12}\text{C}$ targets. The experimental angular distributions for reactions on the ${}^{10}\text{B}$ and ${}^{12}\text{C}$ targets are compared with microscopic DWBA calculations. The shapes of the angular distributions are well described by the calculations and the deduced strength of the effective nucleon-nucleon interaction, V_{11} , is in agreement with previous $({}^3\text{He}, t)$ work.

[NUCLEAR REACTIONS ${}^6\text{Li}$, ${}^{10}\text{B}$, ${}^{12}\text{C}$ $(d, {}^2\text{He})$; $E = 55$ MeV]
 measured $\sigma(\theta)$, ${}^6\text{He}$, ${}^{10}\text{Be}$, ${}^{12}\text{B}$ levels, microscopic
 DWBA analysis, deduced V_{11} .

I. INTRODUCTION

Recently, the feasibility of detecting the unbound ${}^2\text{He}$ system as a nuclear reaction product has been demonstrated in a study of the $(\alpha, {}^2\text{He})$ reaction on several light nuclei.¹ Utilization of this detection system opens up a wide range of new nuclear reactions which can be used for the study of nuclear structure and reaction mechanisms. Among these reactions, that of charge-exchange via $(d, {}^2\text{He})$ is of particular interest because it should be a useful complement to other charge-exchange reactions producing neutron-excess nuclei, such as the (n,p) , $(t, {}^3\text{He})$ and heavy-ion induced reactions, many of which have experimental problems associated with their general application. For example, neutron beams have poor energy resolution and low intensities whereas triton beams are currently only available at moderate energies (< 25 MeV). Though heavy-ion reactions (e.g. $({}^7\text{Li}, {}^7\text{Be})$) are being increasingly employed, the presence of bound excited states of the ejectile frequently complicates the interpretation of the spectra. Since intense high energy deuteron beams are readily available and there are no bound states in ${}^2\text{He}$, the $(d, {}^2\text{He})$ reaction was investigated for its promise as a charge-exchange reaction. In addition, it should be a useful tool for studying neutron-rich nuclei such as ${}^{18}\text{N}$ via the ${}^{18}\text{O}(d, {}^2\text{He}){}^{18}\text{N}$ reaction.

For this initial exploration of the $(d, {}^2\text{He})$ reaction, the $T_z = 0$ targets ${}^6\text{Li}$, ${}^{10}\text{B}$ and ${}^{12}\text{C}$ were bombarded with 55 MeV deuterons. In Sections II and III the ${}^2\text{He}$ detection system and the experimental procedure are discussed. Energy spectra for each target are presented in Section IV and in Section V measured angular distributions for the ${}^{12}\text{C}$ and ${}^{10}\text{B}$ targets are compared with a microscopic DWBA analysis.

II. THE ^2He DETECTION SYSTEM

Since ^2He is unbound, it has to be detected by means of a coincidence measurement of its two breakup protons. Although this detection principle is similar to the one used in detecting the unbound ^8Be nuclide via its two decay α particles,² a difference arises in that the disintegration energy of ^2He does not originate from the breakup of a narrow state, as in the case of ^8Be , but is rather a distribution which results from the 2p-final state interaction. This distribution of the relative energy ϵ of the two protons in their c.m. system has been observed in reactions such as $^2\text{H}(^3\text{He},t)2\text{p}$ (Ref. 3) and is usually described by the theory of Watson and Migdal.⁴ It peaks at $\epsilon \approx 400$ keV and falls off for higher values with a slope of approximately $1/\epsilon$. Therefore the detection geometry was arranged to yield the largest efficiency for this peak value.

The detection of ^2He via its breakup protons with reasonable efficiency is facilitated by the fact that the transformation of the isotropic breakup of ^2He in its c.m. to the laboratory system results in a focussing of the breakup protons into a cone. The maximum opening angle of this cone, β_{max} , is defined by ϵ and the ^2He laboratory energy E and is given by $\beta_{\text{max}} = 2 \arctan (\epsilon/E)^{1/2}$. This transformation also leads to a concentration of breakup protons near the edge of the cone. Therefore, in order to get optimum detection efficiency, it is important that the 2p acceptance angle of the detector be at least as large as the maximum breakup angle which, for example, is 11.4° for $E = 40$ MeV and $\epsilon = 400$ keV. On the other hand, energy resolution considerations require a small horizontal ^2He angular acceptance, in order to minimize kinematic broadening. A good compromise between efficiency and energy resolution was obtained by

detecting the protons in a pair of vertically arranged detector telescopes, thus achieving good efficiency as a result of the large vertical acceptance angle and reasonable energy resolution by limiting the horizontal acceptance angle.

Figure 1 shows a schematic diagram of the detection system which consisted of two large solid-angle counter telescopes collimated by 8 mm wide and 10 mm high slits which were separated by a 10 mm high central post. At 11 cm distance from the target, this system subtended a 15° vertical and a 4° horizontal acceptance angle. The ΔE counters were phosphorus diffused silicon, 380 μm thick, and the E detectors were Si(Li), 5 mm thick, all having the same area of $1 \times 1.4 \text{ cm}^2$. In addition, two 5 mm thick counters were mounted behind the E detectors in order to reject events that traversed the ΔE -E system.

To characterize ^2He events, a subnanosecond fast coincidence between the two ΔE counters and particle identification of the protons in each telescope was required. An electronic time resolution of ~ 200 ps (FWHM) was measured for simulated ^2He events by utilizing a fast risetime pulser and fast/slow preamplifiers. To minimize the charge collection time in the ΔE counters, a high bias voltage (2V/ μm) was maintained. The time-of-flight difference (ΔTOF) spectra of the two protons from the $(d, ^2\text{He})$ reaction were similar to those observed previously from the $(\alpha, ^2\text{He})$ reaction¹ at equivalent ^2He energies. Their half width at half maximum was about 500 ps, which is in good agreement with calculated values. Since the width of a single beam burst was 6 ns, random coincidences were drastically reduced by setting a 1 ns wide window around the ^2He peak in the ΔTOF spectrum. Furthermore, a fast pileup

rejection system was utilized which permitted a high count rate ($32,000 \text{ s}^{-1}$) in each ΔE counter, with an associated system dead time of about 20%.

The overall ^2He detection efficiency is a function of the detector geometry, the relative $2p$ energy ϵ and the ^2He energy E . For the geometry noted above, the efficiency was about 1% for 20-50 MeV ^2He events. This result was calculated with the program EFFCR⁵, which was modified to take into account the distribution of ϵ rather than assuming a fixed breakup energy of 400 keV. Experimental values of ϵ were taken from a study of the $^2\text{H}(^3\text{He}, t)2p$ reaction.³ Breakup energies larger than 3 MeV were not evaluated because the shape of the distribution is not well known in this region; however, only a small fraction of the ^2He events is expected to possess such large breakup energies. Although this uncertainty may introduce a potentially large error in the absolute efficiency, the relative efficiencies are estimated to be accurate to $\pm 5\%$.

III. EXPERIMENTAL PROCEDURE

Self-supporting targets of ${}^6\text{Li}$ (99% enriched, $300 \mu\text{g}/\text{cm}^2$), ${}^{10}\text{B}$ (98% enriched, $155 \mu\text{g}/\text{cm}^2$) and ${}^{12}\text{C}$ (natural, $350 \mu\text{g}/\text{cm}^2$) were bombarded with a 55 MeV deuteron beam from the Lawrence Berkeley Laboratory 88-inch cyclotron. For each target and angle, the maximum beam intensity was limited by the singles count rates in the ΔE counters which determined the dead time of the detection system. Beam intensities ranged from 30 nA at forward angles to 160 nA at backward angles. Typical acquisition times for the spectra shown in Section IV ranged from 2 to 3 hours. The observed energy resolution (400-550 keV FWHM) was determined mainly by kinematic broadening due to the 4° horizontal ${}^2\text{He}$ acceptance angle and the large $dE/d\theta$ for these light targets. In contrast to the $(\alpha, {}^2\text{He})$ reaction,¹ the substantial background observed in these spectra was caused by random two proton coincidences arising from the large proton flux associated with the high energy deuteron beam.

IV. ENERGY SPECTRA

A. The ${}^6\text{Li}(d, {}^2\text{He}){}^6\text{He}$ Reaction ($Q_0 = -4.95$ MeV)

Among the nuclei which may be studied with the $(d, {}^2\text{He})$ reaction, investigations of the ${}^6\text{He}$ nucleus are of particular interest because they offer an opportunity to explore further its relatively poorly known level structure.

At 55 MeV bombarding energy, the ${}^6\text{Li}(d, {}^2\text{He}){}^6\text{He}$ reaction enables one to observe an excitation range in ${}^6\text{He}$ up to 28 MeV, thereby permitting a broad search for highly excited levels in the ${}^6\text{He}$ nucleus. Data from this reaction have been taken at laboratory angles between 17° - 40° . Figure 2 shows the 17° spectrum, in which, except for the ground state transition, no other strong transitions to ${}^6\text{He}$ states are observed. The $(2)^+$ level at 1.8 MeV is rather weakly excited at this angle, however, at 40° it is populated more strongly than the ${}^6\text{He}$ g.s. Although the large peak from the ${}^1\text{H}(d, {}^2\text{He})n$ reaction obscures the ${}^6\text{He}$ excitation range from 4 MeV to 8 MeV at this angle, at the other observed angles there is no evidence for ${}^6\text{He}$ levels in this excitation range. The arrows in Fig. 2 indicate the position of possible transitions to ${}^6\text{He}$ levels which have been previously observed at 13.4, 15.3 and 23.2 MeV. No evidence was obtained for transitions to the 15.3 and 23.2 MeV states at this or other angles; similarly, although possible weak population of the 13.4 MeV state is obscured by a ${}^{12}\text{C}$ contaminant at this angle, no such transitions are observed at other angles.

B. The $^{10}\text{B}(d, ^2\text{He})^{10}\text{Be}$ Reaction ($Q_0 = - 2.00$ MeV)

Although the level structure of ^{10}Be has been investigated with a variety of reactions,⁶ no detailed study of this nuclide with a charge-exchange reaction has been reported so far. Data from the $^{10}\text{B}(d, ^2\text{He})^{10}\text{Be}$ reaction were obtained over a laboratory angular range from 17° to 50° . Figure 3 presents a spectrum from this reaction at 30° . Transitions to the ^{10}Be 0^+ ground state, to the known 2^+ states⁶ at 3.37 and 5.96 MeV and to the 3^- state at 7.37 MeV can be seen. The 2^+ assignment of the state observed at 9.4 MeV is tentative in Ref. 6. Although this reaction covers an excitation range in ^{10}Be up to 25 MeV, no evidence for transitions to states above the 9.4 MeV level was observed above the large continuum.

C. The $^{12}\text{C}(d, ^2\text{He})^{12}\text{B}$ Reaction ($Q_0 = - 14.81$ MeV)

Figure 4 shows a typical spectrum from the $^{12}\text{C}(d, ^2\text{He})^{12}\text{B}$ reaction at the laboratory angle of 50° . Transitions are observed to the known 1^+ g.s. and the 4^- , 4.52 MeV state⁷ and to a previously unknown state at 8.35 ± 0.1 MeV. No evidence for transitions to the 2^+ , 0.95 MeV state is seen at this angle, although it was observed with moderate strength at forward angles. The positions of possible weak transitions to other known states in ^{12}B are indicated.

The $(d, ^2\text{He})$ reaction on ^{12}C preferentially populates the 1^+ ground state of ^{12}B and the 4^- state at 4.52 MeV over the angular range studied (17° - 60° lab.); at the more backward angles, moderate population of the state at 8.35 MeV was observed (see Fig. 4). These results are similar to those observed in a study of the $^{12}\text{C}(n, p)^{12}\text{B}$ reaction at 56 MeV,⁸ where strong transitions to the g.s. and states at 4.4 and 7.8 MeV in ^{12}B have been reported. The latter experiment had very poor energy resolution and

therefore we assume that the states reported at 4.4 MeV and 7.8 MeV correspond to the levels observed at 4.52 MeV and 8.35 MeV in the present experiment. This indicates that the $(d, {}^2\text{He})$ reaction, at comparable beam energies, preferentially populates the same states as does the (n,p) reaction, even though the $(d, {}^2\text{He})$ reaction requires a spin-flip ($S = 1$) transition, whereas in the (n,p) reaction both $S = 0$ and $S = 1$ transitions are allowed.

V. MICROSCOPIC DWBA ANALYSIS

A. Theory

In order to understand the mechanism of the $(d, {}^2\text{He})$ reaction, simple microscopic calculations have been performed. The microscopic interaction formalism has been discussed at length previously.⁹⁻¹¹ In the DWBA formalism the transition amplitude (in obvious notation) is given by:

$$T = \int \chi_f^{(-)*}(\vec{k}_f, \vec{R}') \langle \psi_f | V | \psi_i \rangle \chi_i^{(+)}(\vec{k}_i, \vec{R}') d\vec{R}'$$

where \vec{R}' is a vector between the c.m. of the projectile and the c.m. of the target nucleus. The effective interaction V can be expressed as a sum of nucleon-nucleon interactions:

$$V = \sum_{i=1}^a \sum_{j=1}^A v(\vec{r}_i - \vec{r}_j)$$

where \vec{r}_i and \vec{r}_j are the space coordinates of the projectile and target nucleons and a and A represent the mass number of projectile and target, respectively. Since the $(d, {}^2\text{He})$ reaction introduces both a spin and an isospin flip ($S=T=1$), only the spin and isospin dependent part of the nucleon-nucleon interaction (V_{11}) can contribute. This was assumed to have the following form:

$$v(\vec{r}_i - \vec{r}_j) = V_{11} (\vec{\sigma}_i \cdot \vec{\sigma}_j) (\vec{\tau}_i \cdot \vec{\tau}_j) g(r_i - r_j)$$

For the radial dependence $g(r)$, a Yukawa form with a range α of 1fm^{-1} was used.

If the wave function of the projectile is an S-state, as is assumed in the present study,¹² the nucleon-nucleon interaction can be expressed in terms of an effective projectile-nucleon interaction:¹⁰

$$\bar{V}(\vec{R}', \vec{r}_j) = \int d\xi f^2(\xi) v(\vec{r}_i - \vec{r}_j)$$

where $f(\xi)$ is the internal wavefunction of the projectile. With the Yukawa interaction utilized in this study, the expression for $\bar{V}(\vec{R}', \vec{r}_j)$ is very complex. However, Wesolowski et al.¹³ have shown that this complicated expression can be approximated by a Yukawa potential with the same range α but normalized strength \bar{V} given by:

$$\bar{V} = V \exp(\alpha^2/18\gamma^2)$$

where γ is the average size parameter for the Gaussian wave functions of the projectile and ejectile. Since γ has not been determined for the $(d, {}^2\text{He})$ reaction, it was approximated by $\gamma = 0.402 \text{ fm}^{-1}$ which was calculated for the (d, d') reaction.¹⁰ The effective interaction \bar{V} was extracted using the code DWUCK4 (Ref. 14). For a given single particle transition $j_i \rightarrow j_f$, it calculates σ_{DW} which is related to the differential cross section by:

$$\frac{d\sigma}{d\Omega} = \sum_{\text{LSJ}} (d_i d_f' \cdot C \cdot C' \cdot \bar{V})^2 \cdot \sigma_{\text{DW}}^{\text{LSJ}}$$

where $d_i d_f'$ and C, C' represent target and projectile spectroscopic amplitudes and isospin Clebsch-Gordan coefficients, respectively. The single particle transitions are restricted by the following selection rules¹⁰:

$$|J_f - J_i| \leq J \leq J_f + J_i$$

$$|j_f - j_i| \leq J \leq j_f + j_i$$

$$|l_f - l_i| \leq L \leq l_f + l_i$$

$$|L - S| \leq J \leq L + S$$

$$|T_f - T_i| \leq T \leq T_f + T_i$$

$$\pi_i \cdot \pi_f = (-1)^{l_i + l_f} = (-1)^L$$

The spectroscopic amplitudes \mathcal{S} and \mathcal{S}' for the reactions on ^{12}C and ^{10}B were evaluated using equation A6 in Ref. 10. This equation is basically the product of the coefficients of fractional parentage (CFPs) of the initial and final nuclei summed over all common parent states. For p-shell states the CFPs obtained from the intermediate coupling wave functions of Cohen and Kurath¹⁵ were used. For excited states (denoted*) of the final nuclei only the (A-1) g.s. parent states were considered in the present calculations, since the CFPs for ((A-1) * \otimes p-nucleon) * components of the wave function are not listed in Ref. 15. For sd-shell states, pure jj-coupling wave functions were assumed. The Woods-Saxon optical parameters were $V = 67.4$ MeV, $r_v = 1.25$ fm, $a_v = 0.75$ fm, $W = 10.9$ MeV, $r_w = 1.25$ fm, $a_w = 0.744$ fm, and $V_{LS} = 6.0$ MeV (Ref. 16). For the imaginary potential W, surface absorption was used. The same set was used to describe all deuteron and ^2He channels for both the ^{12}C and ^{10}B targets. Bound state wave functions were calculated using a Woods-Saxon well with a radius of $1.25 A^{1/3}$ fm, a diffuseness of 0.65 fm and a spin-orbit potential of 6 MeV. Well depths were adjusted to give the single-particle binding energies. Finally, the magnitude of V_{11} was obtained by normalizing the calculations to the data.

B. Results and Discussion

Figure 5 shows the experimental differential cross sections for the reaction $^{12}\text{C}(d, ^2\text{He})^{12}\text{B}$ in comparison with the microscopic DWBA calculations. As can be seen, the shapes of the calculated angular distributions are in good agreement with the experimental data for the transitions to the 1^+ , g.s. and the 4^- , 4.52 MeV state of ^{12}B , whereas the transition to the 2^+ , 0.95 MeV state is only described well in the forward angular region. For the g.s. transition, orbital angular momentum transfers of $L = 0$ and $L = 2$ are allowed;

however, the $L = 2$ component contributes less than 10% to the cross section. For the transitions to the 2^+ and 4^- states only $L = 2$ and $L = 3$ transfer are allowed, respectively. The assumed dominant single particle transitions, the dominant allowed orbital angular momentum transfers and the values obtained for the strength of the $S = T = 1$ nucleon-nucleon interaction V_{11} are listed in Table I. It should be noted that these values of V_{11} are in reasonable agreement with $V_{11} = 16.5$ MeV which was deduced for the average value of V_{11} in an extensive study of the $(^3\text{He}, t)$ reaction on several p-shell nuclei.¹¹

Figure 6 shows the experimental and calculated angular distributions for the reaction $^{10}\text{B}(d, ^2\text{He})^{10}\text{Be}$. The shapes of the calculated angular distributions are in good agreement with the experimental data for all observed transitions. For the transitions to the 2^+ states, both $L = 0$ and $L = 2$ transfers were allowed, but as in the $^{12}\text{C}(d, ^2\text{He})^{12}\text{B}$ reaction, the $L = 2$ transfer contributes less than 10% to the cross section. It should be noted that the good agreement between theory and experiment for the angular distribution of the transitions to the 9.4 MeV state corroborates its tentative 2^+ assignment. The values obtained for V_{11} (see Table I) are substantially smaller than those obtained from the $^{12}\text{C}(d, ^2\text{He})^{12}\text{B}$ reaction. These results reflect the fact that the intermediate coupling wave functions for ^{10}B are very complicated and that ^{10}B is poorly described as a $p_{3/2}$ proton coupled to a ^9Be g.s. core, as was assumed in the present calculations.

VI. CONCLUSIONS

The present study demonstrates the utility of employing the $(d, {}^2\text{He})$ reaction as a tool for charge-exchange studies. The good description of the experimental angular distributions by zero-range microscopic DWBA calculations indicates that the $(d, {}^2\text{He})$ reaction is direct; furthermore, this agreement justifies again¹ the assumption that the correlated two-proton system can be described as an unbound ${}^2\text{He}$ particle.

FOOTNOTES AND REFERENCES

†Work performed under the auspices of the U. S. Energy Research and Development Administration.

*On leave from Institut für Strahlen-und Kernphysik, Universität Bonn, Bonn, Germany. Supported by Deutscher Akademischer Austauschdienst.

1. R. Jahn, G. J. Wozniak, D. P. Stahel and J. Cerny, Phys. Rev. Lett. 37, 812 (1976).
2. G. J. Wozniak, N. A. Jelley and J. Cerny, Nucl. Instrum. Methods 120, 29 (1974).
3. B. J. Morton, E. E. Gross, E. V. Hungerford, J. J. Malanify, and A. Zucker, Phys. Rev. 169, 825 (1968).
4. K. M. Watson, Phys. Rev. 88, 1162 (1952) and A. B. Migdal, Zh. Eksperim. i Teor. Fiz 28, 3 (1955). [Translation: Soviet Phys. - JETP 1, 2 (1955)].
5. The program is available from the authors.
6. F. Ajzenberg-Selove, Nucl. Phys. A227, 1 (1974).
7. F. Ajzenberg-Selove, Nucl. Phys. A248, 1 (1975).
8. M. W. McNaughton, N. S. P. King, F. P. Brady and J. L. Ullmann, Nucl. Instrum. Methods 129, 241 (1975).
9. V. A. Madsen, in Nuclear Spectroscopy and Reactions, Vol. D, p. 251, edited by J. Cerny (Academic Press, New York and London, 1975).
10. V. A. Madsen, Nucl. Phys. 80, 177 (1966).
11. G. C. Ball and J. Cerny, Phys. Rev. 177, 1466 (1969).
12. The small D-component of the deuteron wave function was neglected.

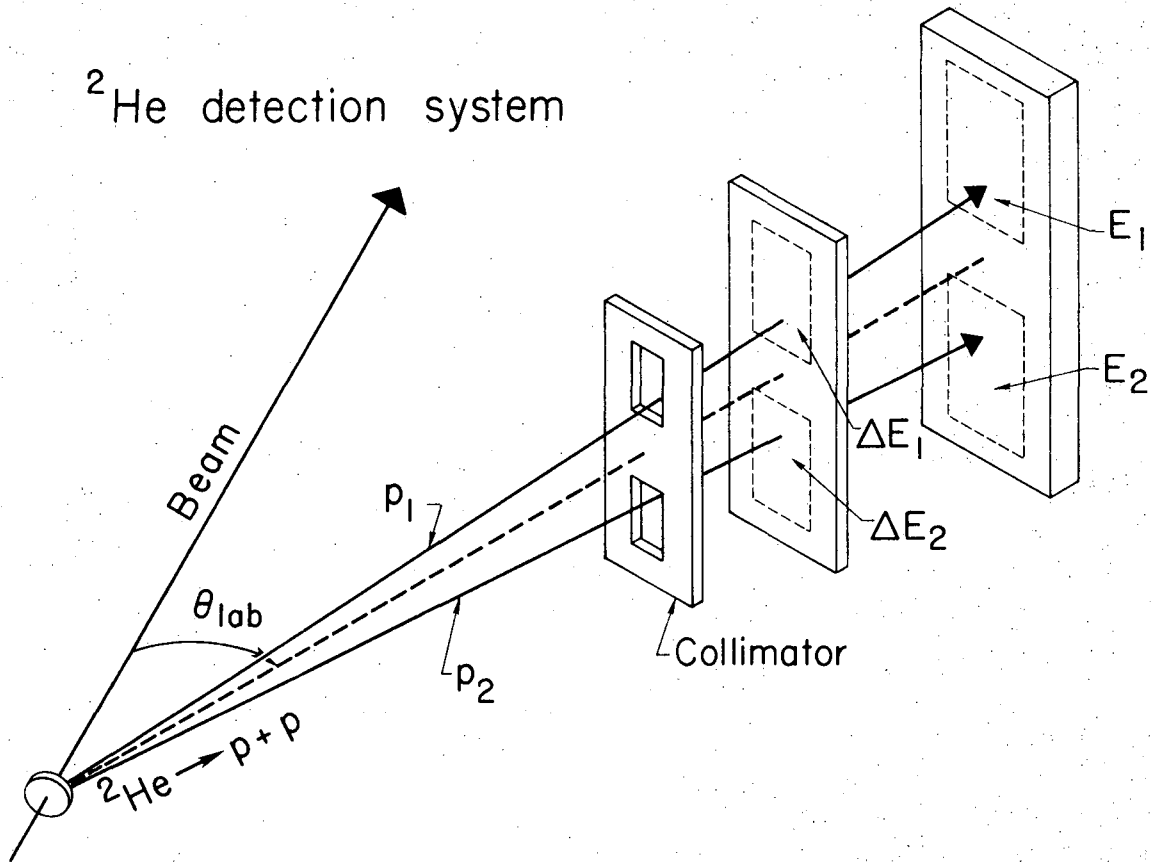
13. J. J. Wesolowski, W. H. Schwarcz, P. G. Roos and C. A. Ludemann,
Phys. Rev. 169, 878 (1968).
14. P. D. Kunz. Computer Code DWUCK4 (unpublished).
15. S. Cohen and D. Kurath, Nucl. Phys. A101, 1 (1967).
16. F. Hinterberger, G. Mairle, U. Schmidt-Rohr, G. J. Wagner and P. Turek,
Nucl. Phys. A111, 265 (1968).

Table I. Deduced strengths of the S=T=1 nucleon-nucleon interaction V_{11} .

Reaction	E_x (MeV)	J^π	Dominant Single-Particle Transition	Dominant L-Transfer	V_{11} (MeV)
$^{12}\text{C}(d, ^2\text{He})^{12}\text{B}$	0.0	1^+	$p_{3/2} \rightarrow p_{1/2}$	0	7.1
	0.95	2^+	$p_{3/2} \rightarrow p_{1/2}$	2	17.0
	4.52	4^-	$p_{3/2} \rightarrow d_{5/2}$	3	6.4
$^{10}\text{B}(d, ^2\text{He})^{10}\text{Be}$	0.0	0^+	$p_{3/2} \rightarrow p_{3/2}$	2	2.3
	3.37	2^+	$p_{3/2} \rightarrow p_{1/2}$	0	0.7
	5.96	2^+	$p_{3/2} \rightarrow p_{1/2}$	0	1.3
	9.4	(2^+)	$p_{3/2} \rightarrow p_{3/2}, p_{1/2}$	0	3.1

FIGURE CAPTIONS

- Fig. 1. Schematic diagram of the ^2He detection system.
- Fig. 2. ^2He energy spectrum obtained from the reaction $^6\text{Li}(d, ^2\text{He})^6\text{He}$ at a deuteron energy of 55 MeV. The arrows indicate the positions of ^6He states previously observed at 13.4, 15.3, and 23.2 MeV.
- Fig. 3. ^2He energy spectrum from the reaction $^{10}\text{B}(d, ^2\text{He})^{10}\text{Be}$ at a deuteron energy of 55 MeV. See text.
- Fig. 4. ^2He energy spectrum from the reaction $^{12}\text{C}(d, ^2\text{He})^{12}\text{B}$ at a deuteron energy of 55 MeV. See text.
- Fig. 5. Absolute differential cross sections for the reaction $^{12}\text{C}(d, ^2\text{He})^{12}\text{B}$ at 55 MeV. Statistical error bars are shown. The solid lines represent microscopic DWBA calculations normalized to the data.
- Fig. 6. Absolute differential cross sections for the reaction $^{10}\text{B}(d, ^2\text{He})^{10}\text{Be}$ at 55 MeV. Statistical error bars are shown. The solid lines represent microscopic DWBA calculations normalized to the data.



XBL 766-2941 A

Fig. 1

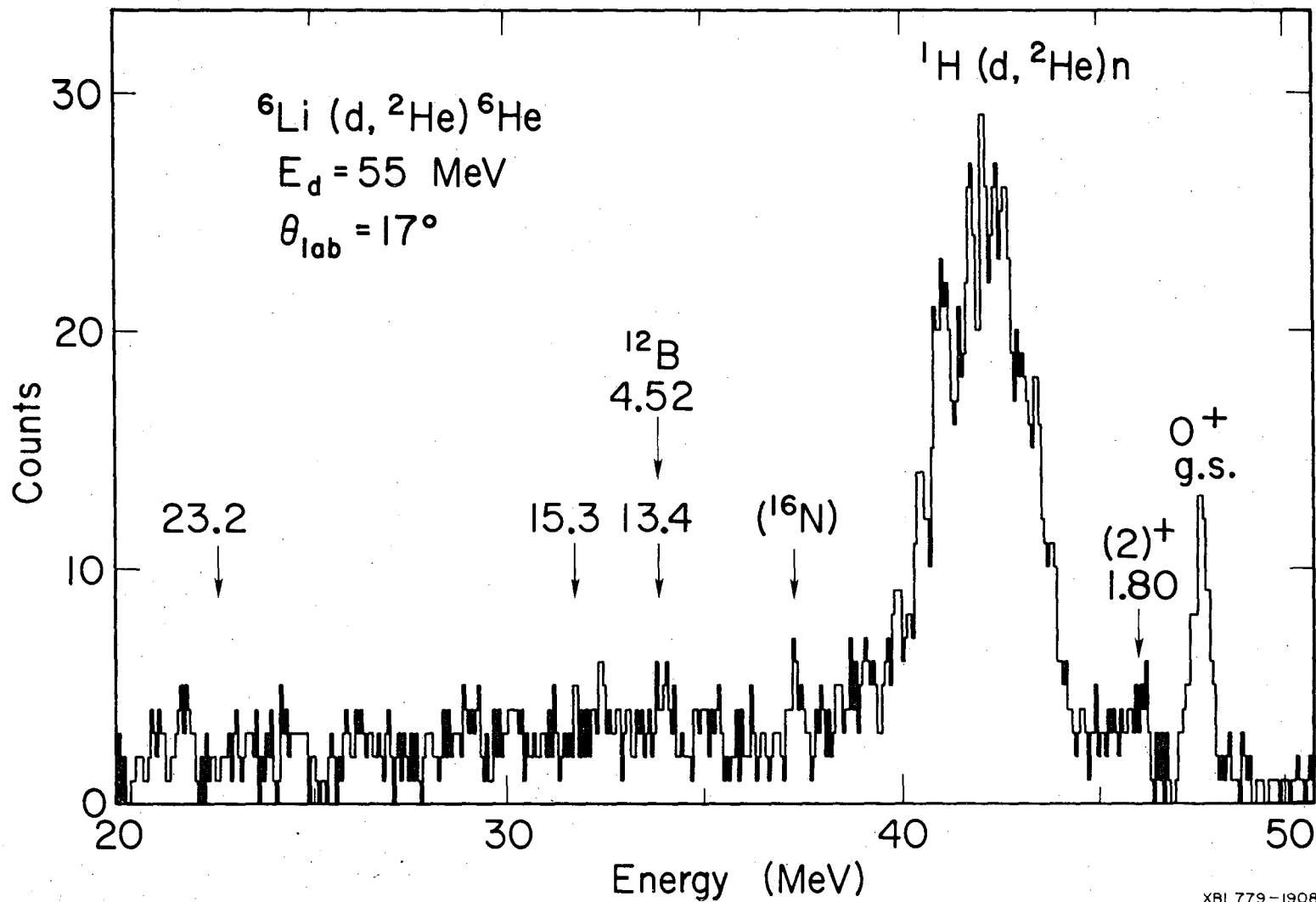


Fig. 2

XBL779-1908

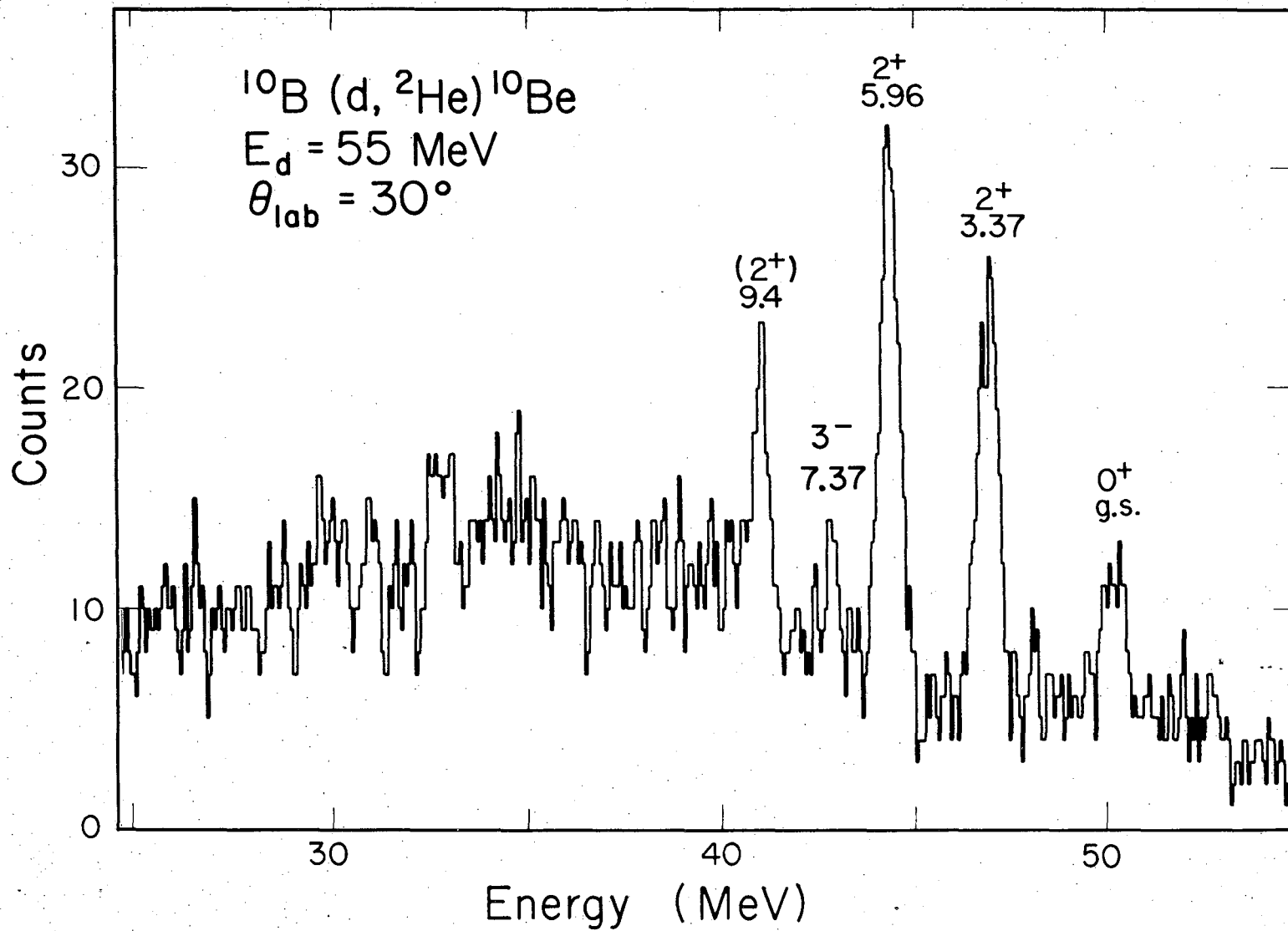


Fig. 3

XBL774-3258

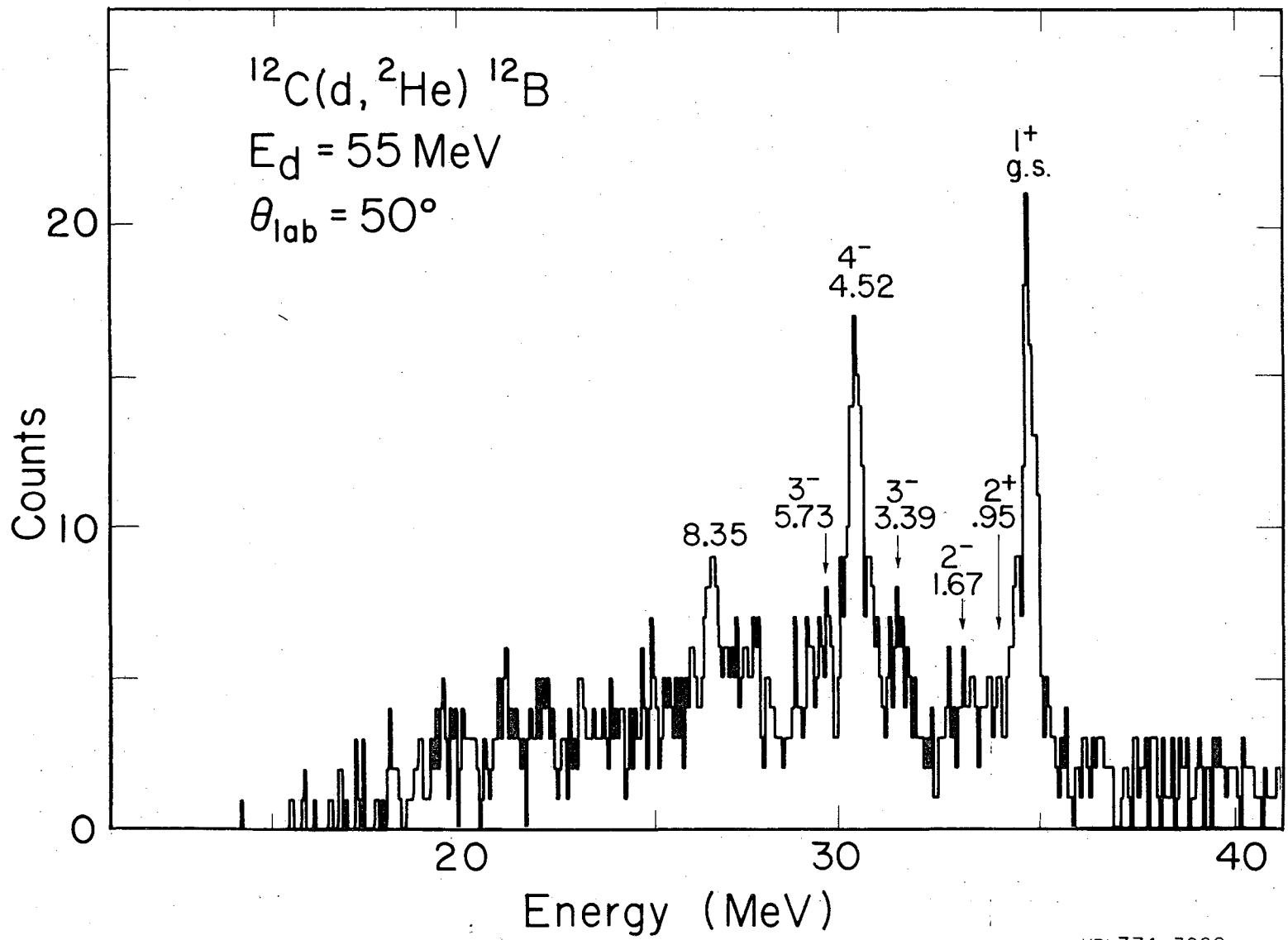


Fig. 4

XBL774-3260

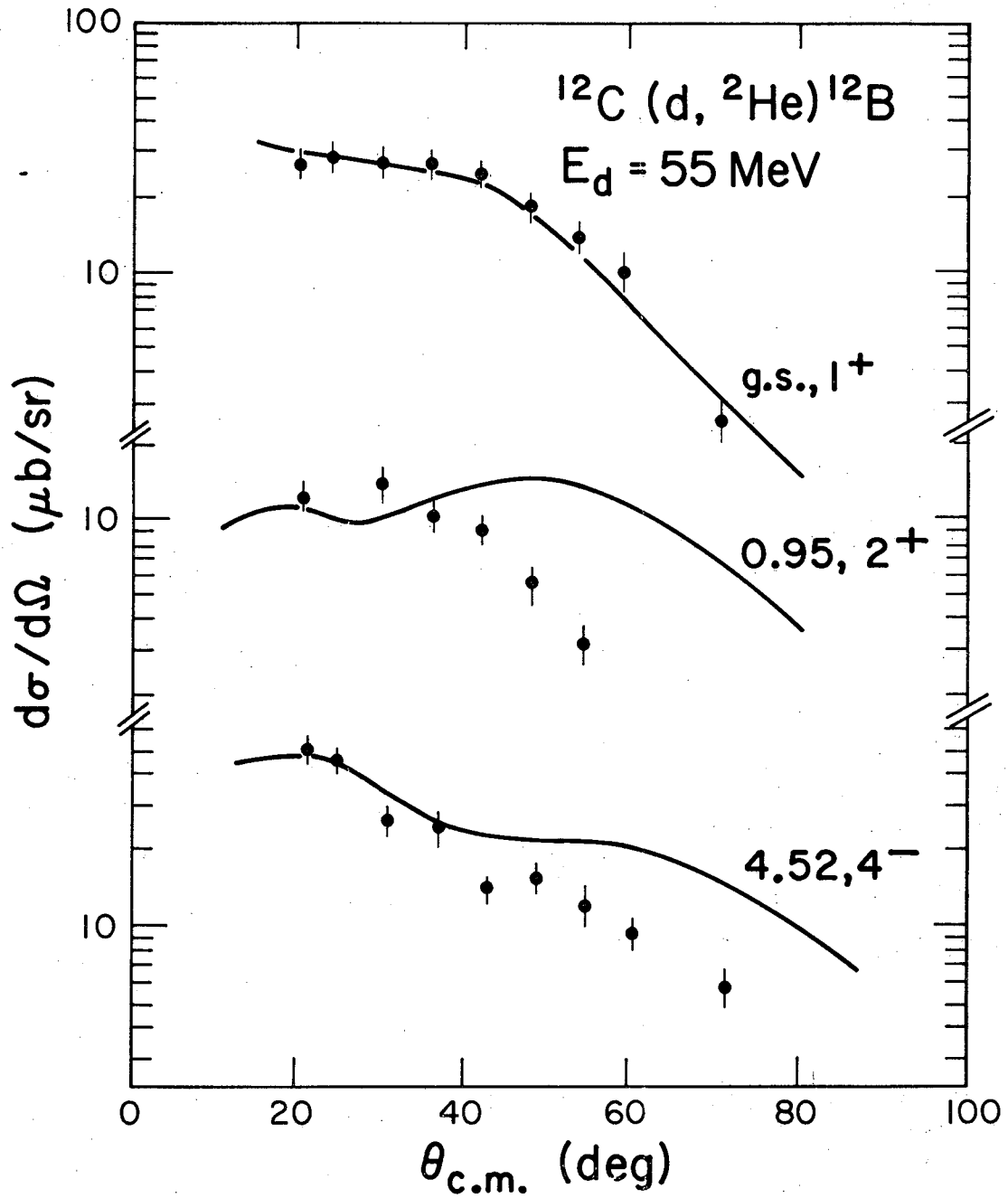


Fig. 5

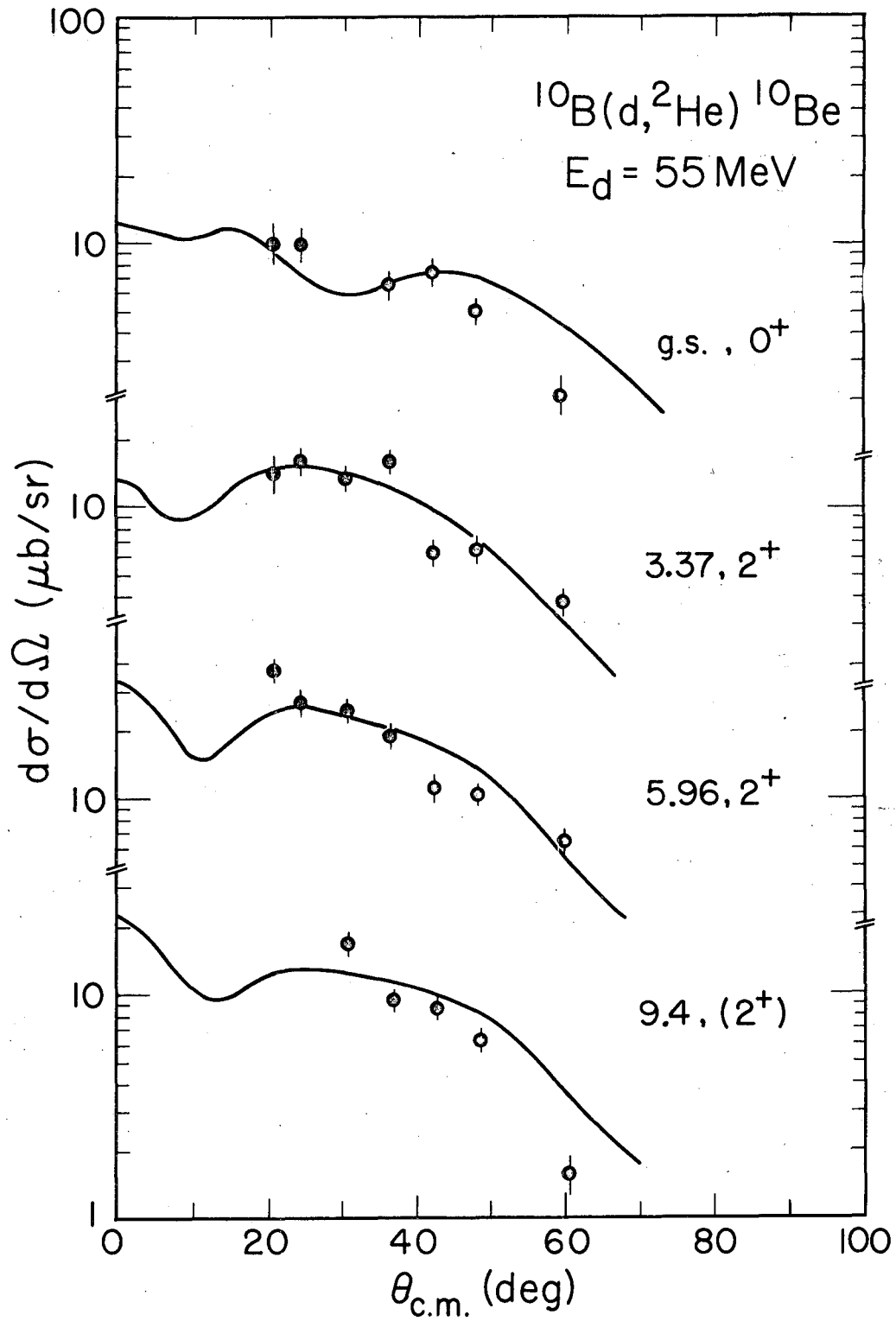


Fig. 6

XBL774-3256

This report was done with support from the Department of Energy. Any conclusions or opinions expressed in this report represent solely those of the author(s) and not necessarily those of The Regents of the University of California, the Lawrence Berkeley Laboratory or the Department of Energy.

TECHNICAL INFORMATION DEPARTMENT
LAWRENCE BERKELEY LABORATORY
UNIVERSITY OF CALIFORNIA
BERKELEY, CALIFORNIA 94720